Acousto-optic interaction in nanodimensional laser heterostructures

Liudmila A. Kulakova

Ioffe Physico-Technical Institute RAS, 26 Polytekhnicheskaya Street, 194021 St. Petersburg, Russia

*Corresponding author: L.Kulakova@mail.ioffe.ru

Received 10 December 2008; accepted 15 January 2009;
posted 29 January 2009 (Doc. ID 105124); published 17 February 2009

Comparative research on fine spectrum analysis techniques (static and dynamic) has been carried out. The advantages of the dynamic method for fine spectrum study of heterolaser radiation as a method of study of the spectrum change under ultrasonic strain have been shown. An approach to fine dynamic spectrum analysis has been developed, and the treatment of experimental data on the spectrum dynamics of the InGaAsP/InP structures in the presence of surface acoustic waves has been carried out. Thus an appreciable contribution of the acousto-optic interaction (comparable with the acousto-electronic interaction), resulting in time modulation of resonance frequencies of the heterolaser optical resonator, was found. The second, no less important, result of the investigation consists of the finding of the possibility to determine phase shifts between acousto-optic and the acousto-electronic interactions.

OCIS codes: 070.1060, 260.3060, 300.6260, 300.6380.

1. Introduction

Tunable mid-IR sources are needed for high-resolution laser spectroscopy and optical communication systems. Currently, one of the most promising optical sources in the mid-IR range is nanodimensional heterolasers operating at room temperature. Their emission wavelengths can be tuned to some extent by electrical heating of the laser's active region [1,2]. Their practical utility depends on how rapidly they can be modulated. Applications such as fast process control or optical FM communication [3] require very fast tuning exceeding that provided by this method. Direct electrical tuning of the optical transition in multisectional lasers [4] or by the Stark effect [5] remains the problem unsolved because the fine spectroscopy application requires continuous frequency tuning and a high level of stability of intensity of laser emission, which are lacking with these methods.

As was recently found, ultrasonic strain can influence the process of optical wavelength emission, thus providing faster time response and more precise wavelength adjustment. This adjustment becomes possible due to acousto-optic and acousto-electronic interactions taking place in the laser heterostuctures. This statement was proved for what we believe to be the first time in our investigations of the influence of alternating strain (produced by bulk ultrasonic waves) on InGaAsP/InP heterolaser emission [6]. The research was carried out for the case of rather unusual conditions of the interactions, i.e., when the acoustic wavelength ($\Lambda_s \approx 400\,\mu$m) was much longer than the aperture ($a \approx 6\,\mu$m) of an optical beam: $\Lambda_s \gg a$. In this case one might expect the interactions to produce a time-dependent change of parameters of a laser cavity and also of an active layer in the laser.

Therefore, one of the goals of this paper was to present new results of a study carried out on the subject. Another goal of the research was to develop the technique of fine spectroscopy. Application of the technique made it possible to reveal changes in the heterolaser emission induced by ultrasonic strain. New data on the emission spectra were obtained using a dynamic method of analysis. The method

0003-6935/09/061128-07$15.00/0

was based on real time spectral measurements by means of a Fabry–Perot etalon (FPE).

2. Experimental Techniques

We have studied InGaAsP/InP laser heterostructures operating at room temperatures at the wavelength of emission $\lambda_m^0 = 1.48\,\mu$m in the pulse mode of operation with a duration time up to $3\,\mu$s. The physical characteristics of the laser structure are described in detail in Refs. [6,7]. The investigation was carried out using a specially designed experimental setup [6,7]. Alternating strain was produced by introduction of a surface acoustic wave (SAW). The Rayleigh SAWs were excited by interdigital transducers (with a resonance frequency of 10 MHz), deposited on substrates made of piezoelectric Y-cut $LiNbO_3$ single crystal. The laser heterostructure was fabricated on the same substrate. The collimated and focused beam of the laser emission was detected by photodiodes with the photocurrent buildup time not exceeding 5 ns. The output signal was amplified (amplifier bandwidth up to 400 MHz) and displayed on a wideband (200 MHz) oscilloscope. Detection of the laser radiation was carried out in three operation modes: using direct measurements, by application of FPE (range of dynamic dispersion 18.25 Å) and applying a monochromator specially modified for detection of pulse radiation.

3. Results and Discussion

In the absence of an acoustic wave, the signal from the emission is a nearly rectangular video pulse. Switching on the ultrasound leads to an almost 100% modulation of the signal amplitude (after FPE) with the periodicity of the acoustic wave. Obviously, the observed modulation of the output signal is due to the changes in the FPE transmission in response to the frequency modulation of the laser emission.

Recall [7] that the straining effects in heterolaser frequency modulation can mainly occur through two mechanisms:

1. The acousto-optic interaction produces a time-dependent modulation of the permittivity and so leads to a change in the resonant wavelengths $\Delta\lambda_R^k/\lambda_R^k = \Delta n_R/n_R$ of the laser optical resonator. Due to the photoelastic effect, the amplitude of the refractive index change in cubic crystals is defined by a relationship $\Delta n_i = -1/2\, n_i{}^3 p_{ij} S_j{}^0$, so

$$\Delta\lambda_R{}^k/\lambda_R{}^k = -1/2\, n_i{}^2 p_{ij} S_j{}^0, \tag{1}$$

where p_{ij} are the photoelastic tensor components and $S_j{}^0$ is the amplitude of an ultrasonic wave. Using the parameters of the crystalline GaAs, $n \approx 3.4$ and $p_{11} = -0.16$. For $S_1{}^0 \approx 10^{-4}$ (at $\lambda_R^k \approx 1.5\,\mu$m), one could calculate for this effect $\Delta\lambda_R^k/\lambda_R^k \approx 0.9 \times 10^{-4}$ and $\Delta\lambda_R^k \approx 1.4$ Å.

2. Similar variations with time, due to the acousto-electronic interaction, associated with the deformation potential constant Λ_j can also occur in the bandgap E_g of the active layer: $\Delta E_g = \Lambda_j S_j$. One might expect this effect to produce a time-dependent change of the gain curve spectral position [7], or the maximum gain wavelength, $\Delta\lambda_m/\lambda_m = -\Delta E_g/E_g$, so that

$$\Delta\lambda_m/\lambda_m = -\lambda_m \Lambda_j S_j/\mathrm{hc}, \tag{2}$$

where h is Planck's constant and c is light velocity. With conventional values of $\Lambda_j = 10$ eV and the same value $S_1 = 10^{-4}$ at $\lambda_m = 1.5\,\mu$m, we obtain $\Delta\lambda_m \approx -18$Å.

Our estimations show that acousto-optic and acousto-electronic effects may differ by an order of magnitude. The sign of their action is determined by the signs of photoelastic (p_{ij}) and deformation potential (Λ_j) constants, respectively.

Understanding of the physical nature of the acousto-optic and acousto-electronic interactions and their relative contribution to the effect of laser wavelength modulation are of importance not only for fundamental knowledge but also for applied science. In order to obtain an efficient and continuous tuning of the laser it is necessary to search for active lasing structures possessing high efficiency as well as equal signs of both acousto-optic and acousto-electronic contributions.

A detailed study of efficiency of the acousto-optic and acousto-electronic interactions should be carried out separately. For this purpose, we used the so-called spectral distribution technique [7], which is nothing but a static version of the spectral analysis. This technique is based on a consideration of the spectrum that is averaged in time. The spectral distribution of light intensity consists of one or several lines (depending on the mode of generation: single frequency or multifrequency). The linewidth is determined by the Q factor, whereas the distance between the lines is determined by the length of the optical resonator of the structure. The intensity of the lines and their quantity are governed by the shape and the width of the gain curve of the laser active layer. In the case of the acousto-optic interaction the introduction of a sound should result in a time-dependent oscillation of the emission lines around the equilibrium spectral positions with the ultrasonic strain frequency. If averaging of the spectrum in time is carried out, then the process results in visible decrease of the spectral line intensities and in the line broadening. It may be expected that a similar effect should be observed in the case of the acousto-electronic interaction. However, in the latter case, the spectral curve of optical gain must be considered in the analysis. As a result one can see a redistribution of the intensities between the spectral lines: a decrease of the central line and an increase of the neighbor line intensities.

The experimental data on the spectral distribution of the laser emission intensity are presented in Fig. 1 (curve 1), where the deviation $\Delta\lambda = \lambda - \lambda_m^0$ is used as

a variable. The switching-on of the SAW (Fig. 1, curve 2) results in the (described above) redistribution of the emission intensity between the lines, while no noticeable line broadening is observed.

A set of Gaussian distributions $I_R(\Delta\lambda, t)$ with the lines of unit intensities was used to describe the lines of a laser resonator. The asymmetry of the gain curve was modeled by a double Gaussian distribution $I_e(\Delta\lambda, t)$. Here we supposed that the envelope of the measured spectrum is uniquely defined by the gain curve. So, the spectral distribution, including strain effects, can be represented in the form

$$I(\Delta\lambda, t) = I_e \times I_R, \tag{3}$$

$$I_R(\Delta\lambda, t) = \sum_k \exp\left(-\frac{2(\Delta\lambda - k\Delta\lambda_R + L_R \mathrm{Sin}\Omega t)^2}{w_R^2}\right), \tag{4}$$

$$I_e(\Delta\lambda, t) = I_0 + A_1 \exp\left(-\frac{2(\Delta\lambda - \Delta\lambda_{m1} + L_e \mathrm{Sin}\Omega t)^2}{w_1^2}\right) + A_2 \exp\left(-\frac{2(\Delta\lambda - \Delta\lambda_{m2} + L_e \mathrm{Sin}\Omega t)^2}{w_2^2}\right), \tag{5}$$

where $\Delta\lambda_R$ is the distance between the optical resonator lines, w_R is their width, I_0 is the background level constant, and $\Delta\lambda_{m1,m2} = \lambda_{m1,m2} - \lambda_m^0$; $\lambda_{m1,m2}$ are the wavelengths of the maxima and w_1 are w_2 are the widths of the corresponding distributions for the gain curve; L_R and L_e are the modulation amplitudes of the resonator lines and the gain curve spectral positions, respectively. It is possible to express them in terms of the frequency modulation amplitudes [7]: $F_R = cL_R/(\lambda_m{}^0)^2$ and $F_e = cL_e/(\lambda_m{}^0)^2$ (c is the velocity of light). The theoretical fit, in accordance with Eq. (3) is presented by curve 3 for the initial state ($L_R = L_e = 0$) in Fig. 1. The following values of parameters were taken for fitting: $I_0 = 0.1$, $A_1 = 11.5$, $w_1 = 5.44$ Å, $\Delta\lambda_{m1} = -0.3$ Å, $A_2 = 2.8$, $w_2 = 6.2$ Å, $\Delta\lambda_{m2} = -7.4$ Å, $\Delta\lambda_R = 3.9$ Å, $w_R = 1.6$ Å, and four lines of the laser resonator ($k = -2, -1, 0, 1$, sufficient for the experiment description) were taken into account.

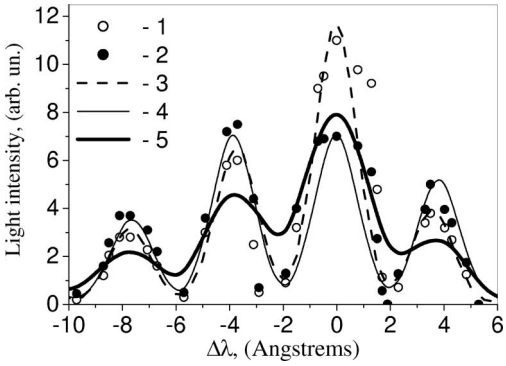

Fig. 1. Spectral distribution of the laser emission intensity. Points, experiment with the SAW switched off (curve 1) and on (curve 2); lines, theoretical calculation: curve 3, equilibrium spectral structure; curve 4, structure arising from acousto-electronic interaction ($L_e = 4.5$ Å); curve 5, structure arising from both acousto-optic ($L_R = 1$ Å) and acousto-electronic ($L_e = 1.2$ Å) interactions.

The spectral distribution change under the ultrasonic strain could be obtained as an average of Eq. (3) over the period of the sound wave:

$$\bar{I}(\Delta\lambda) = \frac{1}{2\pi}\int_{-\pi}^{\pi} I_e(\Delta\lambda, \Omega t) I_R(\Delta\lambda, \Omega t)\mathrm{d}(\Omega t). \tag{6}$$

The best agreement of the experimental data and the results of numerical calculation, using Eq. (6) was observed for $L_e = 4.5$ Å and $L_R \ll L_e$ (Fig. 1, curve 4). This lets one conclude that in the studied structures the acousto-electronic interaction was dominant. It resulted in the modulation of the laser gain curve spectral position in the range of $L_e = \pm 4.5$ Å.

The results presented above show that in the studied structure only intensity redistribution between the lines has been observed. However, the continuous tuning demands a search for structures with a high efficiency of both interactions.

The static method employed so far is a rather tedious procedure, so it seems necessary to develop a universal and mobile technique for the fine spectral analysis of diode laser emission. Dynamic spectral analysis with a FPE seems a promising alternative to the static method.

The dispersion range of the FPE and the set of the orders of transparency are determined by the wavelength and the incidence angle of a light beam. As is well known, a FPE has maxima of transparency when the constructive interference conditions are met. For a monochromatic collimated beam and FPE with an air gap between the mirrors, resonant wavelengths λ^k are determined by the relation

$$\frac{2L_0}{\lambda^k} = k, \tag{7}$$

where $k = 1, 2, \ldots, L_0 - a$ distance between the mirrors of a FPE. On the other hand, various orders n of the interference can be realized for the fixed wavelength λ^k at certain angles θ_{in} of light incidence. At small deviations from the normal propagation ($\theta_i \ll 1$, $L \approx L_0 + \Delta L$) the relation (7) can be transformed as follows:

$$2L_0(1 + 1/2\theta_{\mathrm{in}}^2)/\lambda^k = k + n. \tag{8}$$

One can see that

$$\theta_{\mathrm{in}} = \pm\sqrt{n\lambda^k/L_0}. \tag{9}$$

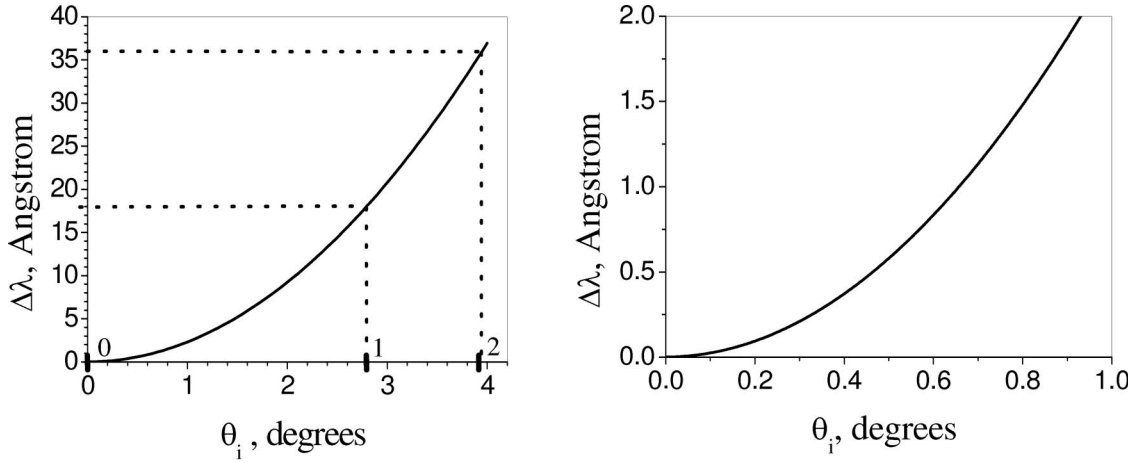

Fig. 2. Dependence of the resonant wavelength change on the FPE rotation angle: in (a) the numbers on the abscissa axis (0, 1, 2) indicate the positions of the angular interference orders; (b) region of small deviations from the normal incidence.

At the same time it is necessary to notice that an increase of the incident angle θ_i leads to an increase of the resonant wavelength λ^k. This circumstance enables one to carry out fine spectral analysis of laser emission within the limits of one angular dispersive range $\theta_{in+1} - \theta_{in}$. A relation between $\Delta\lambda^k$ and θ_i follows from relation (7) (at $\theta_i \ll 1$, $L = L_0 + \Delta L$, $\Delta L \ll L_0$):

$$\Delta\lambda^k = \lambda^k \theta_i^2/2. \tag{10}$$

From the $\Delta\lambda^k(\theta_i)$ dependence (Fig. 2) one can see that by rotating FPE around the zero angle position it is possible to perform a fine analysis of the radiation spectrum to within 0.1 Å.

Experimental dispersion curves (Fig. 3) obtained for the same laser structure ($\lambda_m^0 = 1.48\,\mu$m) show (as expected) a picture that is symmetric about the normal incidence of light. At a laser operation current not much exceeding threshold ($I_{op} < 1.6 I_{th}$), single mode generation is observed at the FPE positions corresponding to different angular interference orders. With the increase of the operating current ($I_{op} \approx 1.7 I_{th}$), in addition to the central line, there appear two neighbor lines of a different intensity. The picture of such spectrum in scaled coordinates ($\Delta\lambda = \lambda - \lambda_m^0$) is presented in Fig. 4 (curve 1). The envelope curve of this spectrum nicely represents the gain curve of the laser [6]. The figure also shows that the width of each of the lines in the emission spectrum is about 1 Å. This means that the interferometer used was characterized by rather high spectral resolution. On the other hand, it may be stated that the lines of emission in the registered lasing spectrum are rather narrow. It is namely in this mode that the spectrum analysis of the straining effect has been performed.

Gaussian approximation according to expressions (3)–(5) was used to describe the spectrum. The most exact agreement with the equilibrium data ($L_e = L_R = 0$) gives the distribution (Fig. 4, curves 2 and 3) with the following parameters:

$$I_0 = 1\,\text{mV}, \quad A_1 = 325\,\text{mV}, \quad \Delta\lambda_{m1} = 0.35\,\text{Å},$$
$$w_1 = 3.73\,\text{Å}, \quad A_2 = 0, \quad w_R = 1\,\text{Å},$$
$$k = -1, 0, 1. \tag{11}$$

Let us analyze the time-dependent SAW-induced change of the emission intensity (past FPE) at different rotation angles of the FPE. The rotation angles are expressed in the resonant wavelength change $\Delta\lambda$.

1. $\Delta\lambda = 0$. At initial state (sound is off) [Fig. 5(a), curve 1], the intensity of transmitted light is a maximum (as expected; see Fig. 4) and nearly constant during the emission pulse. Introduction of the SAW makes the signal oscillate with double periodicity of the sound wave [Fig. 5(a), curve 2]. Such a picture is quite natural, for as was indicated above, acousto-optic and acousto-electronic interactions

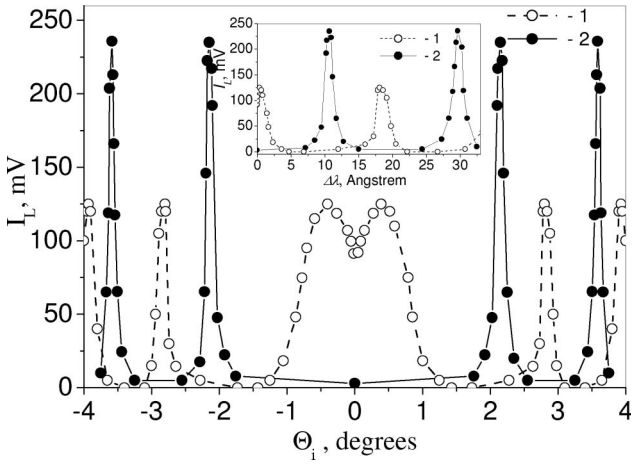

Fig. 3. Dispersive curves of the FPE ($L_0 = 0.6$ mm, $\lambda_0 = 1.48\,\mu$m) obtained for the InGaAsP/InP heterolaser emission at different operating currents: $1 - I_{op} \approx 1.4_{th}$, $2 - I_{op} \approx 1.6 I_{th}$. In the inset on the abscissa axis $\Delta\lambda$ is calculated according to Eq. (10).

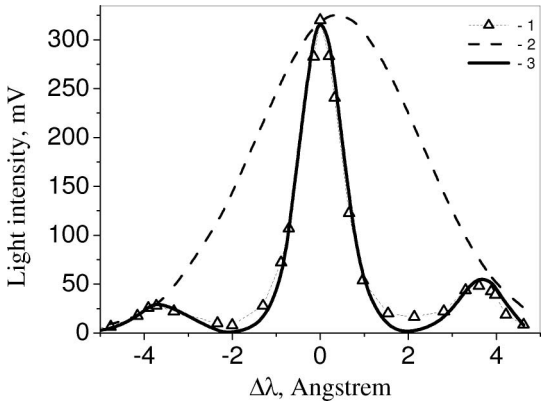

Fig. 4. Spectral distribution of the heterolaser emission intensity, obtained by the FPE: curve 1, experiment; curves 2 and 3, calculation of the laser curve gain and the generated spectrum, respectively.

both lead to a time-dependent modulation of the spectral position of the gain line and the lines of the laser optical resonator.

2. Rotation of the FPE ($\Delta\lambda \neq 0$) leads to a decrease (as expected; see Fig. 4) of the equilibrium signal [Figs. 6(a) and 7(a), curve 1] and to a change in the periodicity and the amplitude of the signal in the presence of the SAW. $\Delta\lambda \approx 1$ Å [Fig. 6(a), curve 2] corresponds to the greatest modulation of the signal with the periodicity of the sound wave and with peak intensity close to that with the FPE in the state of maximum transparency ($\Delta\lambda = 0$) without the strain. At the opposite position $\Delta\lambda \cong -1$ Å [Fig. 7(a), curve 2] the modulation signal [as expected; see Eqs. (3)–(5) and Fig. 4] is in opposite phase in comparison with the previous position ($\Delta\lambda \approx 1$ Å) signal after the FPE.

A slight dissimilarity between Fig. 6(a) (curve 2) and Fig. 7(a) (curve 2) is due to the corresponding asymmetry of the laser gain curve [Fig. 4 (curve 2)].

All measured time-dependent changes of the emission intensity after FPE correlate rather well with the calculated FPE transparency change arising from the respective tuning of the laser emission spectrum with the ultrasonic strain.

Results of the calculation according to Eqs. (3)–(5) with the parameters (11) and at $L_e = 1.2$ Å and $L_R = 1$ Å (curves 2; equilibrium, curves 1) for different $\Delta\lambda$ are presented in Figs. 5(b), 6(b), and 7(b). All these calculations are carried out for the in-phase modulation of the gain curve and lines of the laser resonator. For a comparison with the particular case of the antiphase acousto-optic and acousto-electronic interactions we carried out corresponding calculation for the opposite signs of L_e and L_R. The result of such a calculation [Fig. 7(b), curve 3] contradicts the experimental observation and makes one to conclude of the in-phase action of both interactions in the studied heterolasers.

It is necessary to notice that some (unimportant) discrepancy of the calculation with the experiment (noticeable in particular at $\Delta\lambda = 0$) is the consequence of the assumption of the infinitely narrow structure, i.e., the strain at any fixed moment of time is supposed to be the same across the entire laser resonator. In reality it is not true. We are dealing with a running sound wave and the laser resonator of nonzero width. The mismatch of the experimental situation with the accepted approximation is determined by the ratio of the resonator width and the sound wavelength.

A comparison of $L_e = 1.2$ Å and $L_R = 1$ Å measured experimentally with the values calculated above (representing the same parameters, respectively) $\Delta\lambda_R^k \approx 1.4$ Å and $\Delta\lambda_m \approx -18$ Å leads to the following conclusions.

1. Agreement of the calculated (for the crystalline material) and measured (in a nanodimensional

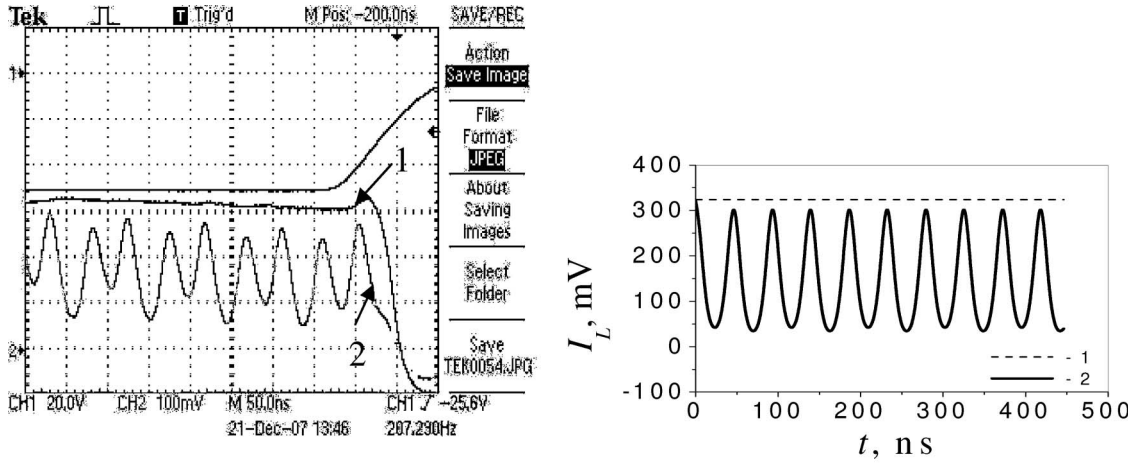

(a) (b)

Fig. 5. (a) Oscillograms ($I_{op} \approx 1.7 I_{th}$): top beam, the operating current pulse; bottom beam, laser emission pulse (the FPE output signal); 1, the sound is absent; 2, in the presence of the SAW ($f = 10.75$ MHz) for $\Delta\lambda = 0$. (b) Dependences of the radiation intensity on time, calculated according Eqs. (1)–(3) with parameters (11) for the equilibrium case (curve 1) and in the presence of the SAW at $L_e = 1.2$ Å, $L_R = 1$ Å (curve 2) for $\Delta\lambda = 0$. The data in (a) and (b) are presented on the same scale.

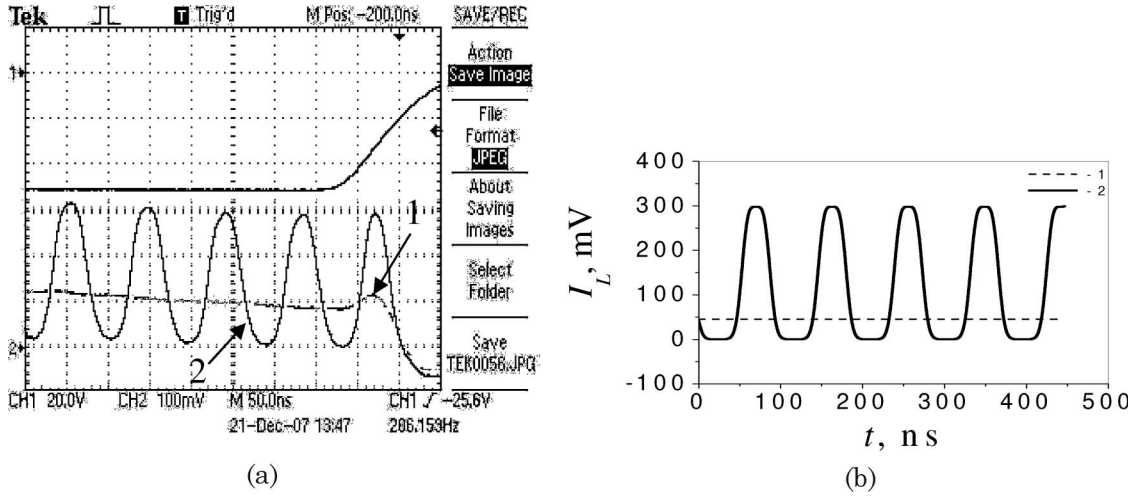

Fig. 6. (a) Oscillograms ($I_{op} \approx 1.7 I_{th}$): top beam, operating current pulse; bottom beam, laser emission pulse (the FPE output signal); 1, the sound is absent; 2, in the presence of the SAW ($f = 10.75$ MHz) for $\Delta\lambda = 1$ Å. (b) Dependences of the radiation intensity on time, calculated according to Eqs. (1)–(3) with parameters (11) for the equilibrium case (curve 1) and in the presence of the SAW at $L_e = 1.2$ Å, $L_R = 1$ Å (curve 2) for $\Delta\lambda = 1$ Å. The data in (a) and (b) are presented on the same scale.

laser heterostructure) acousto-optic efficiencies is rather satisfactory.

2. For the case of the acousto-electronic interaction the calculation predicts larger (almost by an order of magnitude) modulation amplitude. Possible reasons may be (a) the existence of technologically unavoidable mechanical stress of the active layer and (b) less value of $\Lambda_j|\Lambda_j| < 10$ eV in the studied structures.

3. On the other hand, taking into account in-phase action of both interactions in the studied heterolasers we can conclude that [as expected from Eqs. (1) and (2)], in InGaAsP/InP heterostructures both the deformation potential and the photoelastic constant have the same sign, that is, $\Lambda_j < 0$.

Some very important effects were discovered by the dynamic method. In the case of multifrequency generation mode ($I_{op} > 1.7 I_{th}$, large intensity radiation), for what is believed to be the first time it was possible to observe experimentally so-called "burning" of carriers, resulting in an instability of the emission spectrum. At the same time the sound introduction due to the modulation in time of the maximum intensity positions in the laser resonator removes local depletion of carriers. This leads to an increase and stabilization of the mode intensities. Past the FPE one can see an optical signal with stable amplitude, varying in time like the oscillograms in Figs. 5(a), 6(a), and 7(a) show.

Thus, the dynamic spectral analysis not only has shown the basic features and advantages of the method presented here, but also has raised questions concerning some contradictions with the results of the static analysis. Recall that from studying the change of laser spectrum under the ultrasonic strain [7] detected by a monochromator (averaged in time spectrum) we concluded that the acousto-electronic

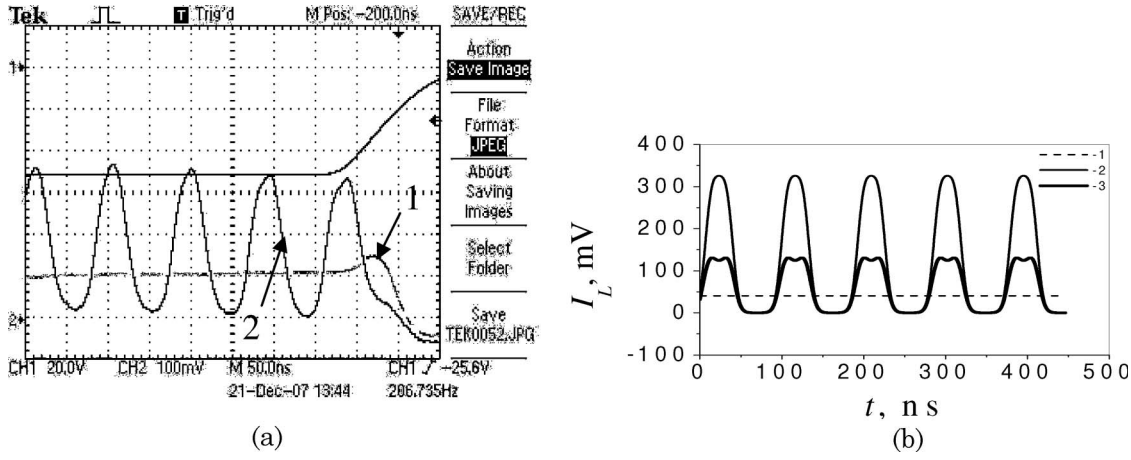

Fig. 7. (a) Oscillograms ($I_{op} \approx 1.7 I_{th}$): top beam, operating current pulse; bottom beam, laser emission pulse (the FPE output signal); 1, the sound is absent; 2, in the presence of the SAW ($f = 10.75$ MHz) for $\Delta\lambda = -1$ Å. (b) Dependences of the radiation intensity on time, calculated according to Eqs. (1)–(3) with parameters (11) for the equilibrium case (curve 1) and in the presence of the SAW at $L_e = 1.2$ Å, $L_R = 1$ Å (curve 2) for $\Delta\lambda = -1$ Å. The data in (a) and (b) are presented on the same scale.

interaction in the studied structures was dominant and resulted in the modulation of the laser gain curve spectral position in the range of $L_e = \pm 4.5$ Å. However, the dynamic analysis has revealed the presence of a commensurable contribution of acousto-optic interaction. Second (no less important) is the disagreement in the quantitative estimations of L_e value.

It is our opinion that (indeed) the fundamental limitations of the static method (revealed by the dynamic analysis) lead to corresponding errors in the fine spectral analysis by this method.

1. A monochromator resolution is less than that of a FPE. As the result, the wavelength modulation of the resonator lines has become irresolvable.
2. The instability of the emission lines (in the multifrequency mode of generation), observable only by the dynamic method, should lead to errors in the spectral distribution of the intensity when averaged over time. The latter, in turn, should result in mistaken measurements of the spectral redistribution under the ultrasonic strain. Really introduction of the ultrasonic wave leads to the improvement of the generation conditions. It results in stabilization and increase of the line intensities. This looks like a growth of the neighboring lines arising from widening of the gain curve in the static analysis of the spectrum.

So, in our opinion, the dynamic method suggested in the paper is the most accurate one for the fine spectral analysis of heterolaser emission.

4. Conclusion

In the research we carried out, new theoretical and experimental results were obtained. The principal results of the dynamic spectral analysis can be stated as follows:

1. The width of the spectral lines of the examined heterolaser cavity is limited to about 1 Å.
2. At the beginning of the over-threshold regime of the laser operation, if the operating current is $I_{op} < 1.6 I_{th}$, only a single spectral line of generation is observed in the emission spectrum.
3. With the increase of the operating current ($I_{op} \approx 1.7 I_{th}$) there appear two neighboring lines of different intensities following the shape of the laser gain curve. The introduction of sound leads to the spectral modulations of both the laser gain curve, and the laser resonator lines positions with periodicity of the sound wave.
4. The observed picture agrees well with the calculation results within the framework of the proposed model with commensurable values of the modulation amplitudes of the resonator lines ($L_R = 1$ Å) and the laser gain curve ($L_e = 1.2$ Å).
5. At the same time it is established that both the acousto-optic and acousto-electronic interactions produce an in-phase action on the studied laser emission spectrum. This means that both the photoelastic and the deformation potential constants have the same signs.
6. Estimation of the frequency modulation amplitude (F_R) results in a value of about 13.5 GHz. This result implies the opportunity for fast and continuous (due to the combined effect of acousto-optic and acousto-electronic interactions) tuning of the emission frequency in the range of 27 GHz on the scale of the ultrasonic wave period.
7. With a further increase of the operating current ($I_{op} > 1.7 I_{th}$) an instability of the emission spectrum is observed. The sound introduction leads to the increase and stabilization of the laser mode intensities. Therefore, the observed effects could lead to a mistaken measurement of the fine spectral distribution when averaged over time by an optical monochromator. This means that the new dynamic technique presented in this paper seems more preferable for a reliable fine spectrum analysis of heterostructure laser radiation.

The authors are grateful to the Russian Program of the Presidium of the RAS, the Russian Foundation for Basic Research (project no. 07-02-00557), and Russian grant SS-2628.2008.2 for financial support.

References

1. L. A. Kulakova, B. A. Matveev, and B. T. Melekh, "Si-Te acousto-optic modulator for 1.7–10.6 mkm IR region," J. Non-Cryst. Solids **266–269**, 969–972 (2000).
2. C. Gmachl, A. Straub, R. Colombelli, F. Capasso, D. L. Sivco, A. M. Sergent, and A. Y. Cho, "Single-mode, tunable distributed-feedback and multiple-wavelength quantum cascade lasers," IEEE J. Quantum Electron. **38**, 569–581 (2002).
3. S. Luryi and M. Gouzman, "Feasibility of an optical frequency modulation system for free-space optical communications," Int. J. High Speed Electron. Syst. **16**, 559–566 (2006).
4. N. A. Pikhtin, A. Yu. Leshko, A. V. Lyutetski, V. B. Khalfin, N. V. Shuvalova, Yu. V. Il'in, and I. S. Tarasov, "Two-section InGaAsP/InP Fabry-Perot laser with a 12 nm tuning range," Tech. Phys. Lett. **23**, 214–216 (1997).
5. S. Suchalkin, M. V. Kisin, S. Luryi, G. Belenky, J. Bruno, F. J. Towner, and R. Tober, "Widely tunable type-II interband cascade laser," Appl. Phys. Lett. **88** 031103 (2006).
6. L. A. Kulakova and I. S. Tarasov, "Heterolaser frequency tuning under the action of ultrasonic waves," JETP Lett. **78**, 67–71 (2003).
7. L. A. Kulakova, N. A. Pikhtin, S. O. Slipchenko, and I. S. Tarasov, "Controlling the radiation spectrum of quantum-well heterostructure lasers by ultrasonic strain," J. Exp. Theor. Phys. **104**, 689–695 (2007).